Aperture-Array & Lens+FPA Multi-Beam Digital Receivers at 28 GHz on Xilinx ZCU 1275 RF SoC

Sravan Pulipati, Viduneth Ariyarathna, Md Rayhan Khan, Shubhendu Bhardwaj and Arjuna Madanayake
Florida International University (FIU), Miami, Florida, USA
{spuli009, pberu002, mkhan118, sbhardwa, amadanay}@fiu.edu

***Abstract* — Emerging mm-wave wireless systems will make extensive use of fully-digital beamforming receivers for achieving highly-directional RF beamformers that are needed for mitigating high path loss in the channel. Two main approaches for achieving multi-beams include aperture-arrays and lenses with focal plane array (FPA) feeds. The paper discusses the realization of 4-element aperture and FPA+lens receivers supporting four RF beams around 28 GHz with 850 MHz of bandwidth per beam. The DSP algorithms operate in real-time on a Xilinx RF SoC device installed on a Xilinx ZCU 1275 evaluation board. Simulated and measured array factors for both aperture-array and lens+FPA digital beamforming receivers are provided.**

***Keywords* — Wireless, mm-wave, beamforming, lens, array.**

I. Introduction

Wireless communications in the mm wave bands require highly directional beams to circumvent high path loss. However, because wavelength reduces with increasing frequency, for a given physical aperture size, the antenna produces gains high enough for maintaining link budgets. Dielectric lens antenna are of great interest in this regard because they allow high gain with beam steerability when fed using a properly designed focal plane array (FPA) feed [1], [2]. The spatial filtering algorithms in conjuction with the FPA feed are used in radio frequency interference mitigation as well [3], [4]. The FPA is located on the focal region of the lens, and is connected to dedicated receivers (or transmitters) that are interfaced to digital radios. Exploiting the high gain lenses along with beam forming abilities of the aperture antennas has critical applications for the upcoming 6G communication links [5]. Here, we explore direct digital beamforming receivers at 28 GHz with up to 850 MHz bandwidth. The two system engineering approaches are explored, namely (1) aperture beamforming which uses a 4-element digital array receiver where discrete Fourier transform (DFT) is used for creating multiple beams from the same aperture and (2) FPA and lens assembly where beamforming is achieved along with high gain supported by a dielectric lens.

In this paper, we report measurements for the first reported fully-digital multi-beam receiver using both aperture and lens based approaches, while making use of the state-of-art Xilinx radio frequency system on chip (RF SoC) devices that have arisen recently as a result of the Defense Advanced Research Projects Agency (DARPA) RF-FPGA program. We implement a beam formed focal plane array consisting of four 1D sub-arrays and a dielectric lens, where digital beam forming is done using Xilinx FPGA RF SoC using a ZCU1275 platform. The digital bemforming on the array aperture allows multiple beams, while lens allows for gain enhancements and directivity improvements for modern 5G/6G applications. Such applications of the RF SoCs are expected to be critically important for future digital mm-wave arrays supporting multiple RF beams with enhanced flexiblity due to their integrated approach of combining high-speed data converters with field programmable gate array (FPGA) reconfigurable logic fabrics. For example, DARPA's MIDAS program is dedicated to real-time mm-wave digital multi-beam beamforming [6]. In our paper, we discuss how the most advanced digital-RF technology available to us is utilized to achieve fully-digital mm-wave multi-beams in real time.

II. Multi-Beam Digital Beamforming

The use of aperture arrays allows maximum flexibility in digital beamforming. Nevertheless, sharp beams (i.e., high gain) can only be achieved with large numbers of antennas and their dedicated transceivers making aperture arrays a relatively high-complexity (also higher cost) approach. We propose to experimentally verify 28 GHz receivers by first obtaining a 4-element fully-digital receiver array based on a uniform linear array of elements on a 0.75λ uniform spacing. The receivers are of direct-conversion type with 800 MHz of IF bandwidth and 24 dB of gain. We employ a spatial FFT based beamforming approach to generate multiple simultaneous beams. Later, we explore using the 4-element aperture array as a feed array for a high-gain dielectric lens antenna. The use of the lens allows sharper beams due to the inherent high-gain arising from the larger physical aperture of the lens, albeit at the same degrees of freedom as the original aperture array, since the number of degrees of freedom depends only on the number of independent channels (i.e., four).

A. Lens Antenna Design

Hemispherical lens with cylindrical base was designed by first determining the aperture area of the lens based on the desired directivity of 29 dBi and then by calculating the height of cylindrical section based on known dielectric constant of the printing material ABS. Lens radius r = 5 cm was used to obtain a directivity $D = 10log(4\pi \times 2\pi r^2/\lambda^2)$ to be 29.3 dBi for λ = 10.7 mm at 28 GHz (Fig. 1(a)). Hemispherical lens is indeed an approximation of ellipsoidal lens with antenna positioned at the focus. Referring to [7], length of the base is calculated to be L = 5.7 cm using following design equations,

$$L = b\frac{1+\frac{1}{n}}{\sqrt{1-\frac{1}{n^2}}} - r \quad \text{where } b = r(1+\frac{1}{3n^2}). \tag{1}$$

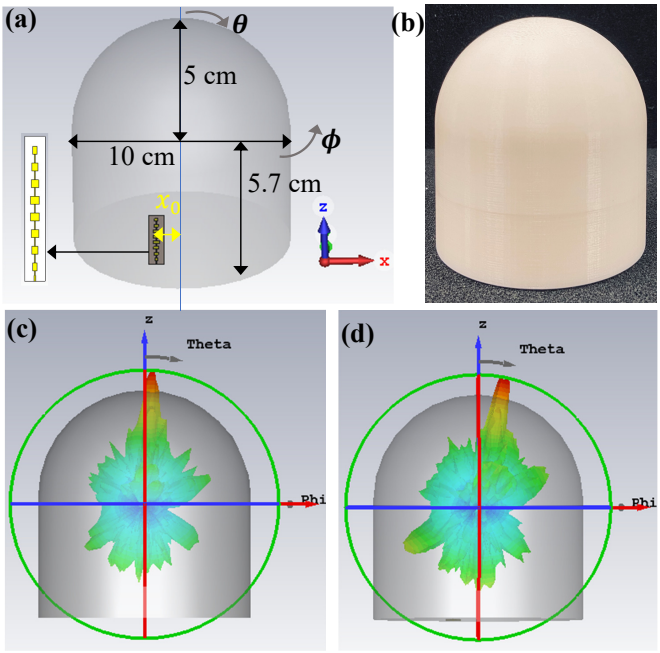

Fig. 1. Validation of the lens + 1D array using full-wave electromagnetic simulations using CST. (a) Designed lens structure along with dimensions. Parameter x_o was varied as x_o = -12, -4, 4, 12 mm to emulate the beams radiated by the four 1D arrays. (b) 3D printed lens used for measurements. 3D beams with peak at θ = 4^o, 12^o resulting due to x_o = 4 and 12 mm are shown in (c) and (d) respectively. For x_o = -12, -4 mm cases beams in opposite directions were obtained (not shown).

Here $n = \sqrt{\epsilon_r}$ is the refractive index of the ABS material chosen to be 1.581, as per ϵ_r = 2.5.

The performance of the array and lens structure was then evaluated using full-wave electromagnetic simulation as shown in Fig. 1 (a). Beam steering is made possible by changing the position of the 1D array x_o, which emulates the excitation of two of the four 1D arrays implemented in the patch array. The beam position by considering other two position x_o= -4 and -12 mm (not shown in figure) are found to be at symmetrically elevation angles. Simulation and measurement results of the patch antennas with lens is further shown and discussed in Fig. 1(c) and (d).

B. Pattern Synthesis

In a lens antenna with N feed antenna elements in the FPA, each feed element produces its own high-gain far-field beam, with pattern denoted as $f_k(\theta, \phi, x, y) \in \mathbb{C}, k = 1, 2, ..., N$, where $(\theta, \phi) \in \mathbb{R}^2$ are angles in vertical and horizontal planes, and $(x, y) \in \mathbb{R}^2$ is the location of the feed element on the focal plane, respectively. The above model shows that the lens pattern depends on the location of the feed antenna. A uniform linear array FPA fixes one of the spatial coordinate to be constant, say $x = x_0$ and places each feed element on a uniformly spaced linear grid, such that $x = (k-1)\Delta x$. Typically, $\Delta x = \lambda/2$. Linear combination of FPA signals using either digital signal processing or analog/microwave circuits between the beams of the PAF elements results in flexible beam synthesis in the far-field. Let $\alpha_k \in \mathbb{C},\ k = 1, 2, ..., N$

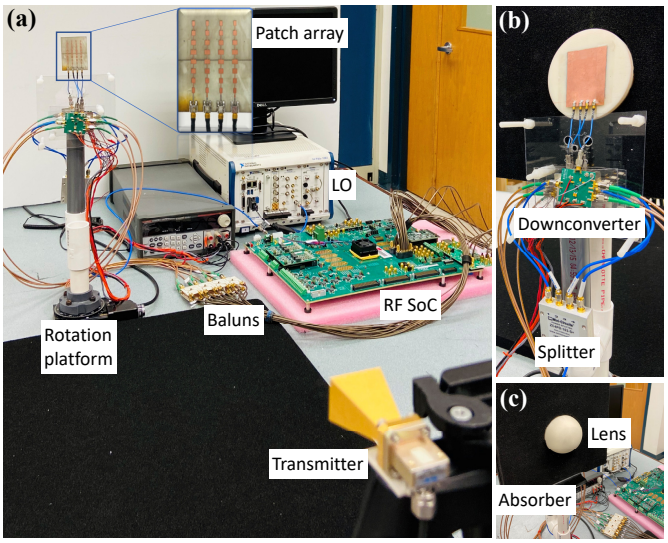

Fig. 2. (a) Experimental setup with digital back-end RF SoC system and local oscillator (b) Receiver chains for the 4-element FPA (and aperture array) with array taped to the base of the ABS plastic lens. The LO is split 4-ways using a microwave divider network. (c) Front view of lens+FPA.

be the weights applied to each beam. The far-field beam pattern is $F(\theta, \phi, x_0, x_0) = \sum_{k=1}^{N} \alpha_k f_k(\theta, \phi, x_0 + (k-1)\lambda/2, x_0) e^{-j\pi(k-1)\sin\phi} \in \mathbb{C}$ assuming the FPA elements are placed at $\lambda/2$ spacing in air, and angles are measured from the array broadside direction. Although the FPA interacts with the dielectric lens and the antennas are completely embedded in the dielectric, our mathematical model ignores the lens geometry and electromagnetic parameters; it models each element as a unique complex-valued far-field pattern.

III. Hardware Setup using Xilinx ZCU1275

A 28 GHz 4-element receiver array is designed using commercial-off-the-shelf (COTS) components for aperture and lens multibeam measurements. The entire experimental receiver setup is shown in Fig. 2. The following sections describe briefly the details of the antenna array, receiver chain and digital back-end. Extensive design details of the hardware setup aren't included due to page limitation and can be found in [8].

A. Antenna Array

The 4-element patch antenna array shown in Fig. 2(a) is used for both digital aperture and lens beamforming, where it acts as the FPA for the latter case. We designed the 4-element array to operate at 28 GHz with 850 MHz of bandwidth as per the 5G standards [9]. Each individual antenna has been built as an 8-element series fed vertical sub-array to provide higher gain in the elevation plane to aid the real-time beam measurements.

B. Receiver Chains

A down converter chip from (Analog Devices HMC1065LP4E) with a conversion gain of 9 dB and noise figure (NF) of 3 dB is employed to mix down to

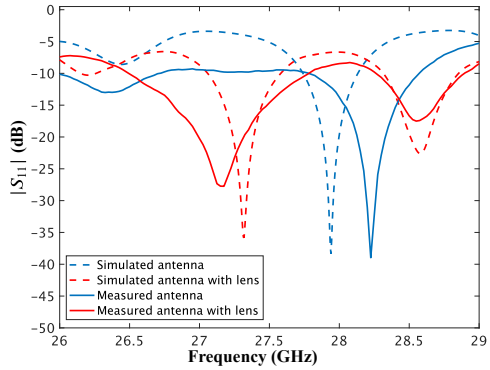

Fig. 3. Return loss for the designed patch 1D array with and without lens.

baseband (up to about DC-1 GHz). The down converter module HMC1065LP4E incorporates a frequency doubler and therefore, the LO input can be driven at half the frequency of the RF band. A centralized LO distribution network is used to simultaneously and coherently drive all the channels from the array. The I-Q downconverted signals are converted to differential from single-ended using baluns (MiniCircuits TCM2-33WX+) in order to interface with the balanced inputs on the Xilinx RF-SoC ADCs.

C. Digital Back-End

The digital back-end of the system is implemented using Xilinx ZCU1275 [10] development platform which incorporates a Zynq UltraScale+RFSoC [11]. Both aperture and lens+FPA beamformers use the same receivers and RF SoC platform. In addition to a high-capacity field programmable gate array (FPGA) fabric, the Xilinx RF SoC XCZU29DR chip in the ZCU 1275 board contains 16, 2 GSps ADCs having a resolution of 12-bits and 16, 6.4 GSps DACs of 14-bit resolution, all integrated into a single integrated circuit. The array receiver uses 8 ADC channels in the RF SoC to synchronously sample the 4 IQ IF signal pairs from the 28 GHz antenna front-ends in order to perform digital signal processing (DSP) in real-time. In the experiments, the IF signals are connected to the data converters of the Xilinx RF SoC which are configured to sample at 1966.08 MHz. A polyphase architecture containing 8 parallel cores is employed for digital designs to accommodate the 850 MHz bandwidth. Therefore, the inbuilt FIFOs of the XDCIP core was configured to output a sample rate of $1966.08/8 = 245.76$ MSps rate with 8 sampled words per clock edge streamed into the digital beamforming cores. The outputs of each first in first out (FIFO) clocked memory stream are synchronized to a single reference clock at 245.76 MHz that was derived from the analog sampling clock. The calibration mode of each ADC channel was set to "Mode-2" [12] in the XDCIP. The ADC calibration is handled by the start-up finite-state-machine inbuilt in the XDCIP. Calibration of the RF front-ends were performed digitally by imposing gain and phase correction. The gain phase mismatches were pre-measured using a reference signal with respect to one receiver chain. This was done by employing a complex multiplier at each phase of each channel.

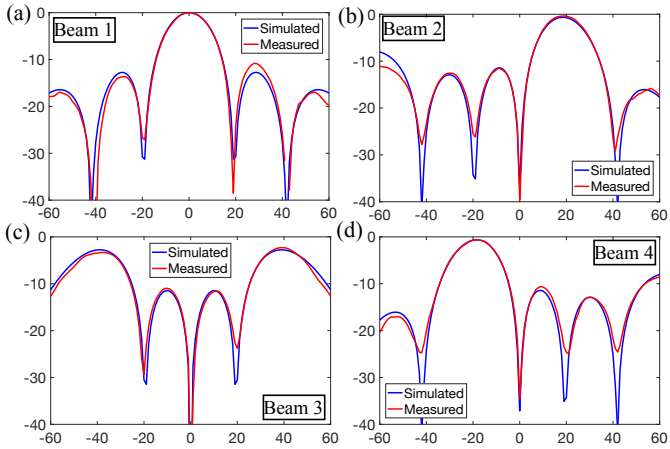

Fig. 4. (a-d) Aperture array 4-beam real-time digital beamforming at 28 GHz. Simulated and measured beam patterns corresponding to each output of the FFT multi-beam beamformer at $f_{IF} = 100$ MHz. The y-axis : array factor gain in dB and the x-axis : azimuth angle.

IV. Experimental Results

A. Antenna Reflection Coefficient Measurements

The measured and simulated reflection coefficient (S_{11}) for 1D array with and without lens are shown Fig. 3. As noted, the resonant frequency of the patch array is found to have shifted up from 28 GHz to 28.25 GHz in fabricated prototype due to uncertainty in the thickness and dielectric constant of the substrate. Furthermore, upon introduction of the lens, we notice decrease in the resonant frequency of the resonant mode. This is due to increase in the dielectric of the medium around the antenna. A new resonant modes at 28.5 GHz is also developed due to introduction of lens, but is also noted in full-wave simulations, suggesting sanity of the measurements.

B. Aperture and Lens Multibeam Measurements

In the transmitter receiver setup shown in Fig. 2, a horn-antenna is used as the transmitter to send test signals centered across the 28 GHz band. The frequency of the LO input to the receivers was set to 13.95 GHz so that after the frequency doublers, the LO signal is set to 27.9 GHz. This allows to bring down the RF center frequency to baseband zero. For beam measurements, the angle of arrival of the incident wave was slowly varied by rotating the receiver array.

1) Measured Aperture Multibeams (without lens)

Four simultaneous receive-mode RF beams were realized by using a 4-point FFT digital core across the spatial samples realizing the 4-simultaneous beams. The beamformed outputs of each beam of each phase is used to compute the received energy for each direction of arrival using digital integrators. The bandwidth per beam was about 800 MHz. Fig. 4 shows the simulated and measured array factors for the 4-beam digital beamformer for IF=100 MHz. Simulated array factors are generated from fixed point simulations of the 4-point FFT design in Matlab Simulink, and they do take the element pattern into effect. The plots convey that the measured beams from all 4 bins of FFT agree quite well with the simulated beam patterns at the emulated IF frequency of 100 MHz.

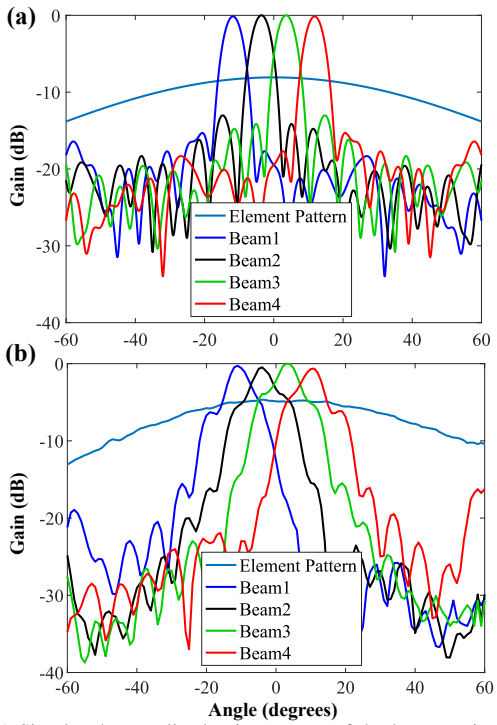

Fig. 5. (a) Simulated normalized gain patterns of the beams using full-wave electromagnetic simulation using CST. Elemental subarray gain pattern (normalized by the maximum of beam pattern) is shown for comparison. (b) Measured normalized gain patterns of the beams extracted from RF SoC and corresponding normalized elemental subarray pattern.

2) *Measured Lens+FPA Beams*

In Fig. 5(a) we show the normalized gain patterns of the lens and array configuration using the simulation set-up shown in Fig. 1. The elemental pattern (1D patch subarray without a lens) is also shown showing the relative gain improvement due to introduced lens. Similar beam patterns and elemental subarray patterns were also extracted from the RF SoC. For this measurement, the LO was set to 27.9 GHz at mixer to provide 100 MHz IF signal. Fig. 5(b) shows the corresponding measurements obtained from the Xilinx RF SoC ZCU 1275 digital platform, where it independently received and integrated the samples from each of the receivers connected to the FPA at the base of the lens. There is good agreement in the position of the beam in elevation space when we compare simulation and measurement results.

We note a gain enhancement of 8 dB due to lens placed over the patch array. This gain is much smaller than the anticipated gain of the lens, since the theoretical design equations of the lens assumed an isotropic point source positioned at the focus of the lens. In practice, due to its high gain, 1D subarray's focal point lies behind the base of the lens and should be adjusted to match with lens' focal point. These effects were not considered in current work and will be part of our future work. Furthermore, comparing the simulated and measured peak gain values, we note a 2 to 3.5 dB difference between the simulated and measured data. We expect these differences to be due to (1) material losses in ABS material, which are not accounted for in the simulation model and (2) due to uncertainties in the knowledge of dielectric constant which is reported to be between 2.5 to 3.0 in prior literature. Consideration of these effects will further improve the effectiveness of the lens design and will be the subject of future work.

V. Conclusions

The paper describes the first reported fully-digital multi-beam digital beamformer at mm-wave. The experiments prove the practical feasibility of aperture- and lens-based fully-digital multi-beams at 28 GHz with more than 800 MHz of bandwidth per beam using DSP on a Xilinx RF SoC device. Design equations, models, and measured array patterns for both aperture and lens based digital beamforming receivers are provided thus exemplifying the practicality of high-bandwidth real-time multi-beam fully-digital base-stations for emerging mm-wave/5G and 6G wireless applications.

Acknowledgment

The authors are grateful to the US National Science Foundation (NSF) for supporting this work.

References

[1] D. B. Hayman, T. S. Bird, K. P. Esselle, and P. J. Hall, "Experimental Demonstration of Focal Plane Array Beamforming in a Prototype Radiotelescope," *IEEE Transactions on Antennas and Propagation*, vol. 58, no. 6, pp. 1922–1934, June 2010.

[2] A. Sayeed, C. Hall, and K. Y. Zhu, "A lens array multi-beam mimo testbed for real-time mmwave communication and sensing," in *Proceedings of the 1st ACM Workshop on Millimeter-Wave Networks and Sensing Systems 2017*. ACM, 2017, pp. 35–40.

[3] C. K. Hansen, K. F. Warnick, B. D. Jeffs, J. R. Fisher, and R. Bradley, "Interference mitigation using a focal plane array," *Radio Science*, vol. 40, no. 05, pp. 1–13, Oct 2005.

[4] J. R. Nagel, K. F. Warnick, B. D. Jeffs, J. R. Fisher, and R. Bradley, "Experimental verification of radio frequency interference mitigation with a focal plane array feed," *Radio Science*, vol. 42, no. 06, pp. 1–8, Dec 2007.

[5] A. Bisognin, N. Nachabe, C. Luxey, F. Gianesello, D. Gloria, J. R. Costa, C. A. Fernandes, Y. Alvarez, A. Arboleya-Arboleya, J. Laviada, F. Las-Heras, N. Dolatsha, B. Grave, M. Sawaby, and A. Arbabian, "Ball grid array module with integrated shaped lens for 5g backhaul/fronthaul communications in f-band," *IEEE Transactions on Antennas and Propagation*, vol. 65, no. 12, pp. 6380–6394, Dec 2017.

[6] "Millimeter Wave Digital Arrays." [Online]. Available: https://www.darpa.mil/program/millimeter-wave-digital-arrays

[7] W. B. Dou and Z. L. Sun, "Ray Tracing on Extended Hemispherical and Elliptical Silicon Dielectric Lenses," *International Journal of Infrared and Millimeter Waves*, vol. 16, no. 11, pp. 1993–2002, nov 1995. [Online]. Available: http://link.springer.com/10.1007/BF02072553

[8] S. Pulipati, V. Ariyarathna, U. De Silva, N. Akram, E. Alwan, A. Madanayake, S. Mandal, and T. S. Rappaport, "A Direct-Conversion Digital Beamforming Array Receiver with 800 MHz Channel Bandwidth at 28 GHz using Xilinx RF SoC," in *2019 IEEE International Conference on Microwaves, Antennas, Communications and Electronic Systems (COMCAS)*. IEEE, 2019, pp. 1–5.

[9] "FCC establishes procedures for first 5G spectrum auctions," Federal Communications Commission: Public Notice (FCC 18-109), Aug. 2018, Available: https://docs.fcc.gov/public/attachments/DOC-353228A1.pdf.

[10] Xilinx, "ZCU1275 Characterization Board User Guide (v1.0)," Nov. 2018. [Online]. Available: https://www.xilinx.com/support/documentation/boards_and_kits/zcu1275/ug1285-zcu1275-char-bd.pdf

[11] Xilinx®, "Zynq UltraScale RFSoC Data Sheet DC and AC Switching Characteristics," Available: https://tinyurl.com/yc728o6x.

[12] Xilinx, "Zynq UltraScale+ RFSoC RF Data Converter 2.0," Apr. 2018. [Online]. Available: https://www.xilinx.com/support/documentation/ip_documentation/usp_rf_data_converter/v2_0/pg269-rf-data-converter.pdf